

# Retrieval of aerosol and volcanic ash properties from Raman lidar with optimal estimation

Adam C. Povey<sup>1</sup>, Roy G. Grainger<sup>1</sup>, Daniel M. Peters<sup>1</sup>, Judith L. Agnew<sup>2</sup>, David Rees<sup>3</sup>

<sup>1</sup>Atmospheric, Oceanic, and Planetary Physics, University of Oxford, UK

<sup>2</sup>STFC Rutherford Appleton Laboratory, Harwell, UK

<sup>3</sup>Hovemere Ltd., Tonbridge, UK

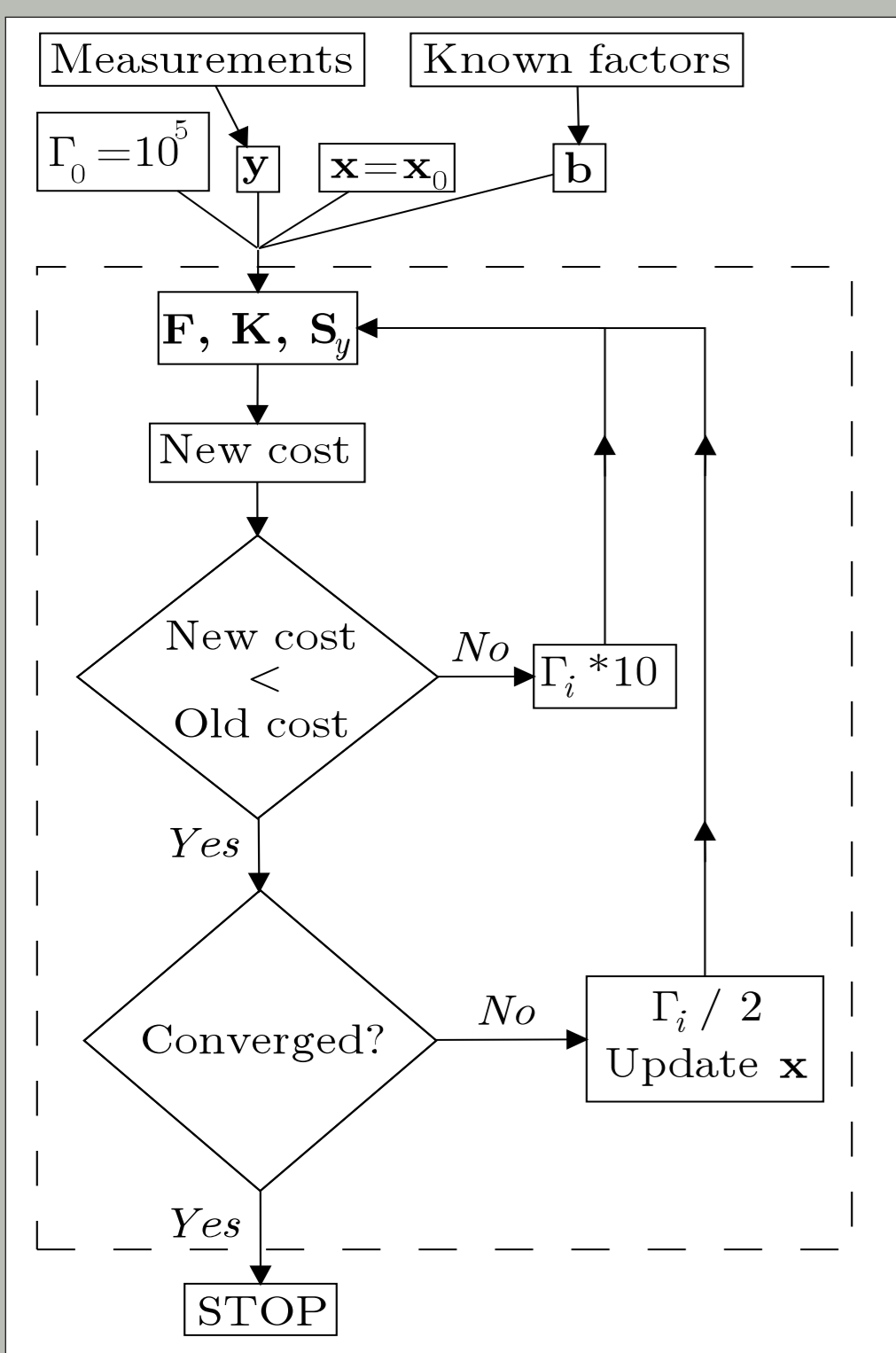


## Motivation

Aerosols impact the Earth's radiation budget both directly, by reflecting solar radiation back into space, and indirectly, by altering the properties and distribution of clouds or reacting with other species. Lidar is an active remote sensing technique that observes the distribution of molecules and particles in the atmosphere as a function of height by means of the light they backscatter from a laser beam. Despite its exceptionally high spatial and temporal resolution, lidar is not as widely applied as other techniques in the study of aerosol.

Optimal estimation retrieval, a form of non-linear regression, has been successfully applied to the analysis of radiometer, radar, and other observations but has not seen substantial use within the lidar community. Such a retrieval processes all measurements simultaneously, making optimal use of the information available and choosing the most appropriate vertical resolution for the result while fully characterising the covariant uncertainty due to measurement noise, model error, and other assumptions. This paper applies the technique to the estimation of aerosol extinction and backscatter from two-channel Raman lidar observations.

## Optimal estimation



A schematic of the optimal estimation algorithm.

As outlined in [1], optimal estimation solves the inverse problem,

$$\mathbf{y} = \mathbf{F}(\mathbf{x}, \mathbf{b}) + \epsilon,$$

where  $\mathbf{y}$  contains the measurements with noise  $\epsilon$  and the forward model  $\mathbf{F}(\mathbf{x}, \mathbf{b})$  translates a state of the atmosphere, summarised by unknown parameters  $\mathbf{x}$  and known parameters  $\mathbf{b}$ , into a simulated measurement.

The cost of a solution (e.g. probability that the system has a state  $\mathbf{x}$  given the measurement  $\mathbf{y}$ ) can be written as,

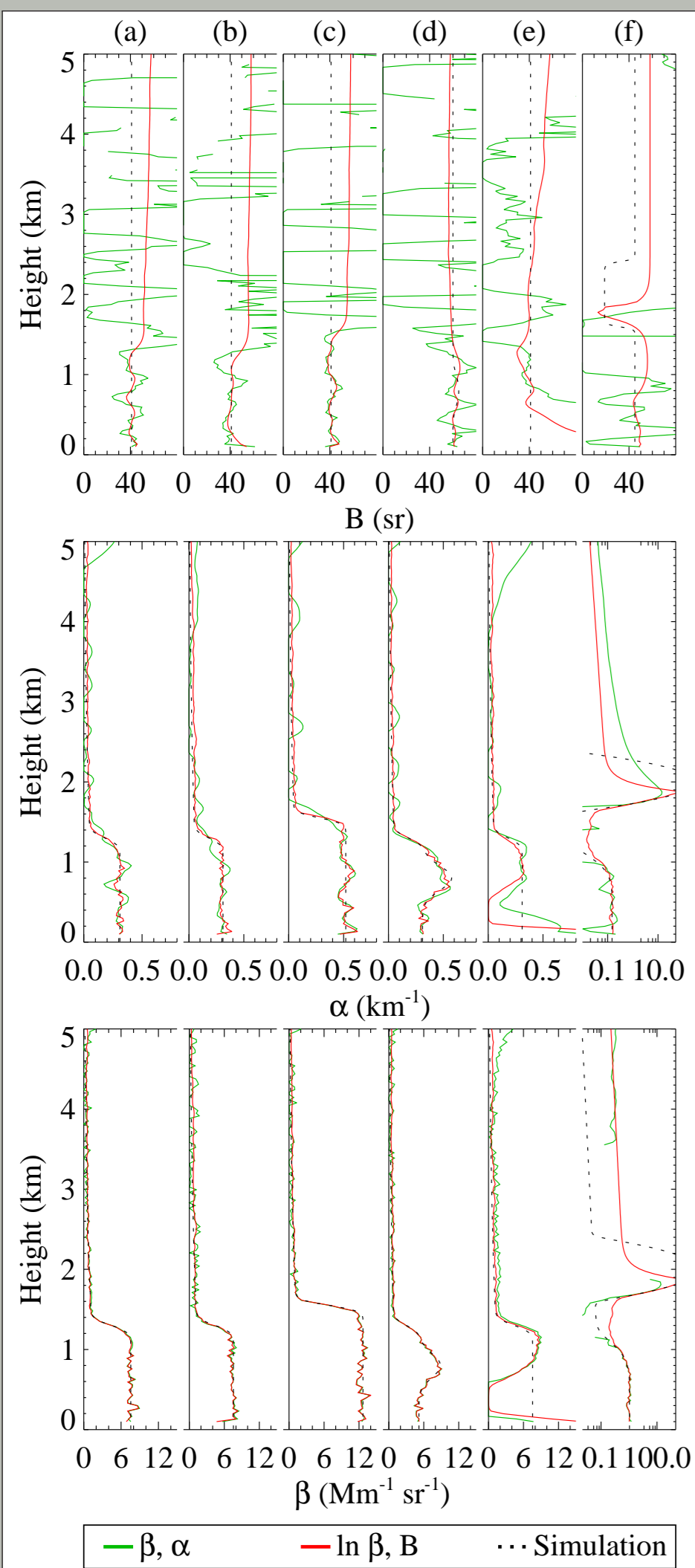
$$[\mathbf{y} - \mathbf{F}(\mathbf{x}, \mathbf{b})]^T \mathbf{S}_y^{-1} [\mathbf{y} - \mathbf{F}(\mathbf{x}, \mathbf{b})] + [\mathbf{x} - \mathbf{x}_a]^T \mathbf{S}_a^{-1} [\mathbf{x} - \mathbf{x}_a],$$

where the covariance matrix  $\mathbf{S}_y$  summarises the uncertainty in both the measurement and parameters while  $\mathbf{x}_a$  is the *a priori* state with covariance  $\mathbf{S}_a$ . It can then be shown that the iteration,

$$\mathbf{x}_{i+1} = \mathbf{x}_i + [(1 + \Gamma_i) \mathbf{S}_a^{-1} + \mathbf{K}_i^T \mathbf{S}_y^{-1} \mathbf{K}_i]^{-1} \{ \mathbf{K}_i^T \mathbf{S}_y^{-1} [\mathbf{y} - \mathbf{F}(\mathbf{x}_i, \mathbf{b})] - \mathbf{S}_a^{-1} (\mathbf{x}_i - \mathbf{x}_a) \},$$

converges to the minimal cost (most probable) state  $\hat{\mathbf{x}}$ , where the  $\mathbf{K}_i = \nabla_{\mathbf{x}} \mathbf{F}(\mathbf{x}_i, \mathbf{b})$  and  $\Gamma_i$  is a scaling constant.

## Simulations



Retrievals from six simulated cases (dashed) when retrieving backscatter and extinction (green) or log backscatter and lidar ratio (red).

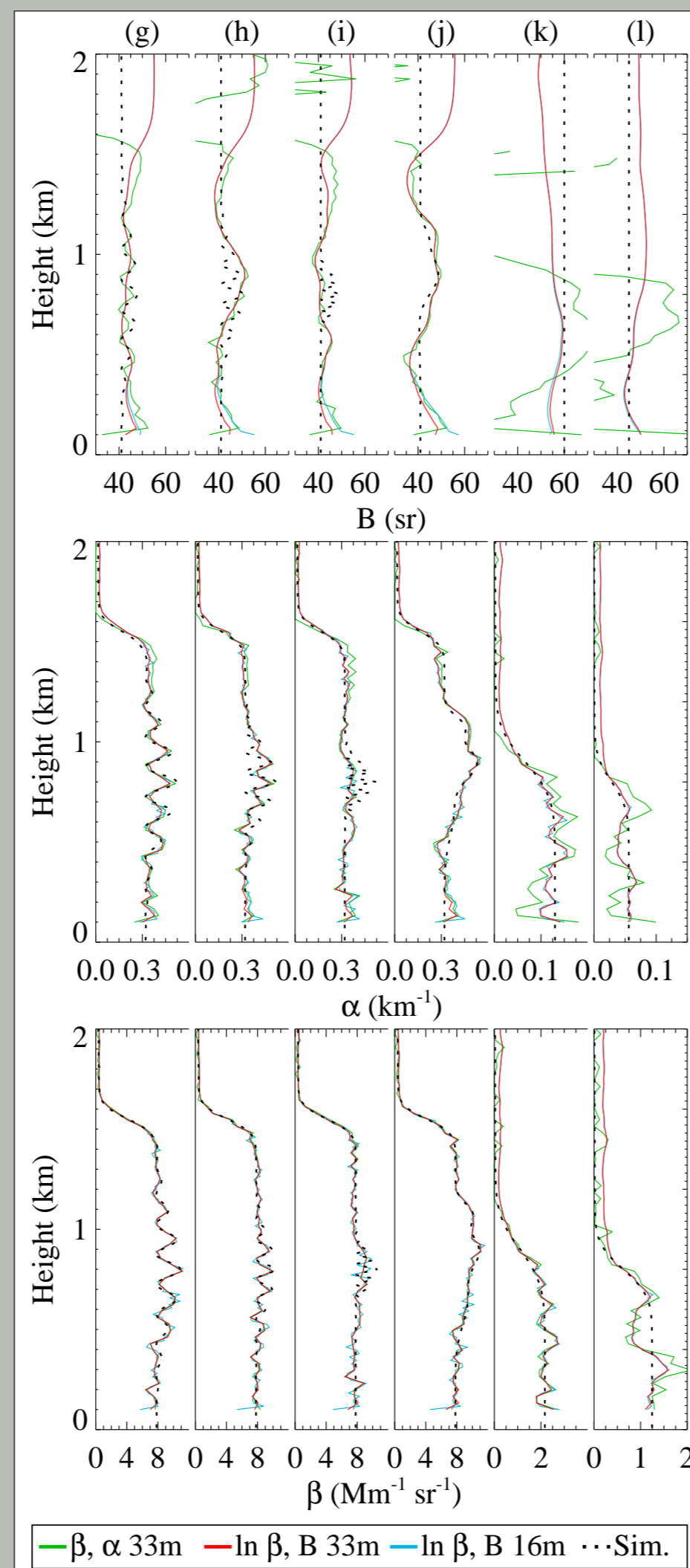
The forward model is designed to retrieve aerosol backscatter ( $\beta$ ) with either extinction ( $\alpha$ ) or the lidar ratio ( $B$ ). The profiles retrieved by either configuration from six simulations are shown left. Both successfully reproduce the simulated profile in cases (a–d). Cases (e) and (f) return large costs indicating a failed retrieval. In (e), a nonlinearity in the detector results in an underestimation of the scattering. Case (f) is reasonable within the planetary boundary layer (PBL) but fails where scattering within a cloud falls outside of the range prescribed by the aerosol-based *a priori*. Successfully fitting cloud and aerosol observations simultaneously requires a more detailed forward model and *a priori*.

The lidar ratio profiles indicate there is decreased information content above

the PBL. There, the lidar ratio configuration relies on its *a priori* value, returning a smooth (but inaccurate) lidar ratio profile while the extinction configuration gives a much noisier profile, indicating it is less constrained.

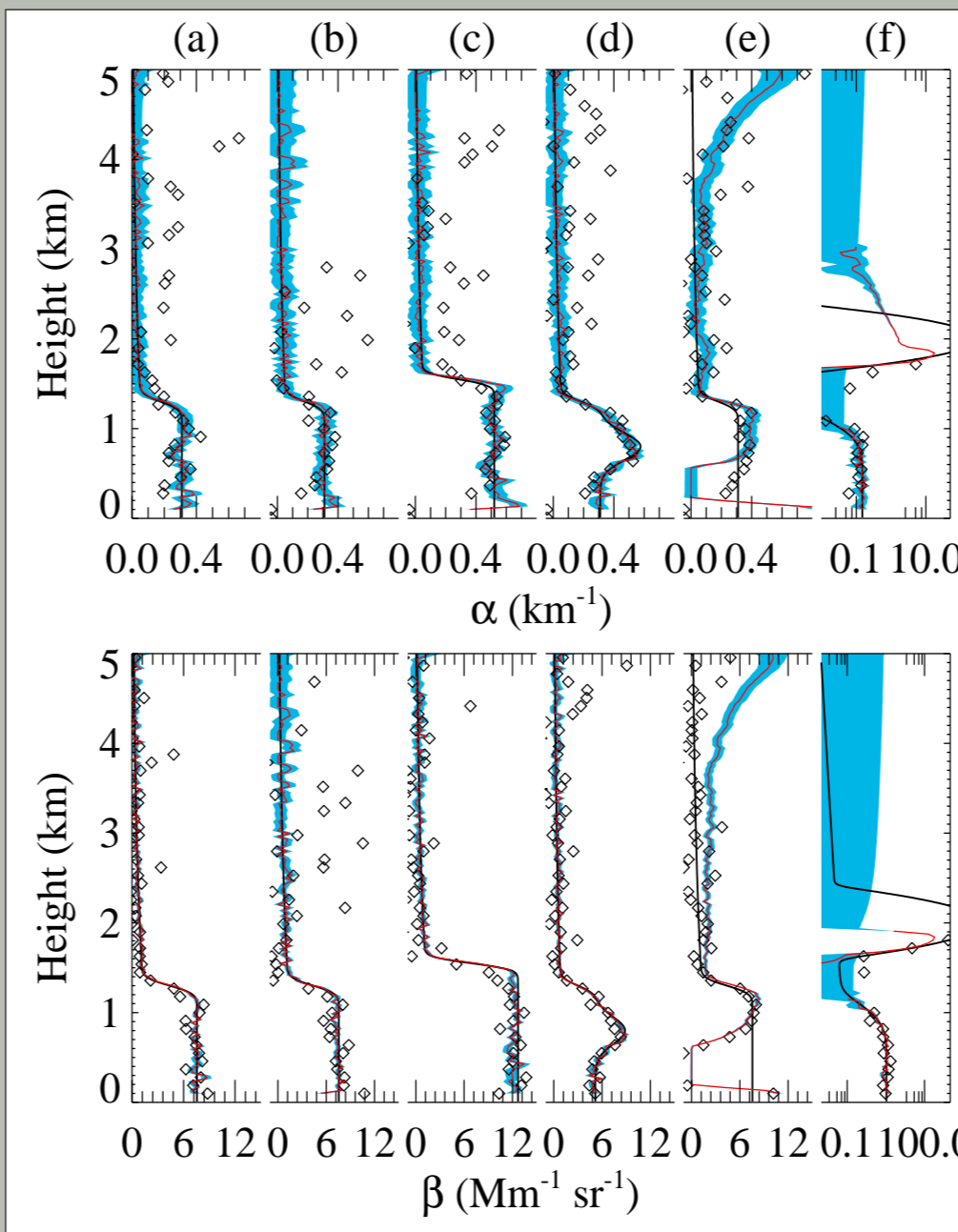
Six further simulations which include small-scale fluctuations are presented right. The lidar ratio mode still returns a smoother profile that loses sensitivity above the PBL. The 'layers' of cases (g) and (h) are correctly positioned by both modes, but those of case (i) are not resolved as they occupy only one retrieval bin. Doubling the resolution gives equivalent performance to before but with slightly increased noise and significantly increased processing time. Cases (k) and (l) are more difficult retrievals as they present lower SNR but still reproduce the true profile.

The resolution of these products can be estimated by the width of the rows of the averaging kernel,  $\mathbf{A} = (\mathbf{K}^T \mathbf{S}_y^{-1} \mathbf{K} + \mathbf{S}_a^{-1})^{-1} \mathbf{K}^T \mathbf{S}_y^{-1} \mathbf{K}$ . Though the backscatter kernels are virtually delta functions ( $\sim 30$  m resolution), the extinction and lidar ratio kernels have widths of  $\sim 300$  m. These widen above the PBL by approximately an order of magnitude. Overall, the kernels indicate that the smoother profiles returned by the lidar ratio mode are due to a greater reliance on the *a priori*.



As left, but for six more complex cases. The retrieval of log backscatter and lidar ratio at twice the original resolution is shown in blue.

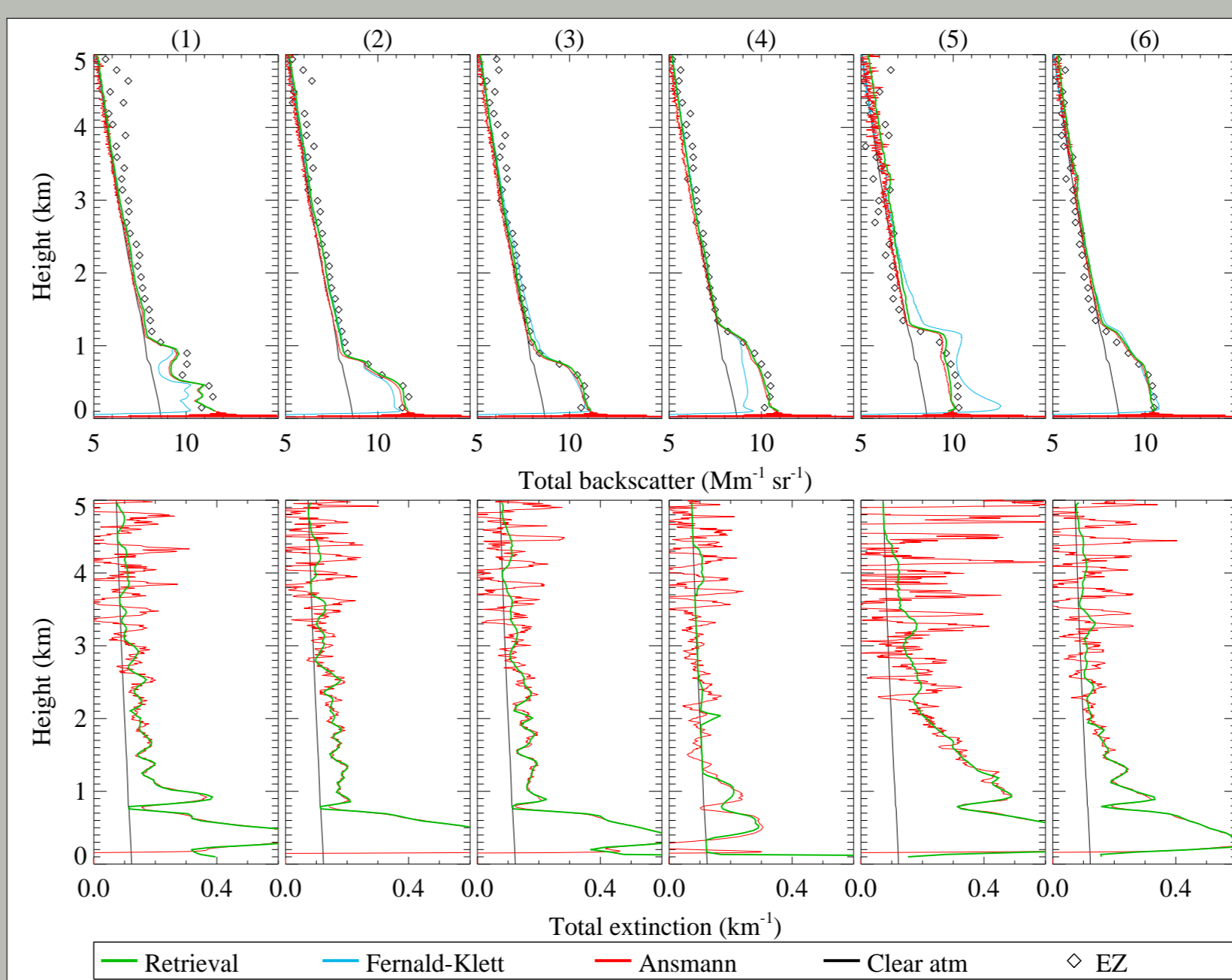
## Uncertainties



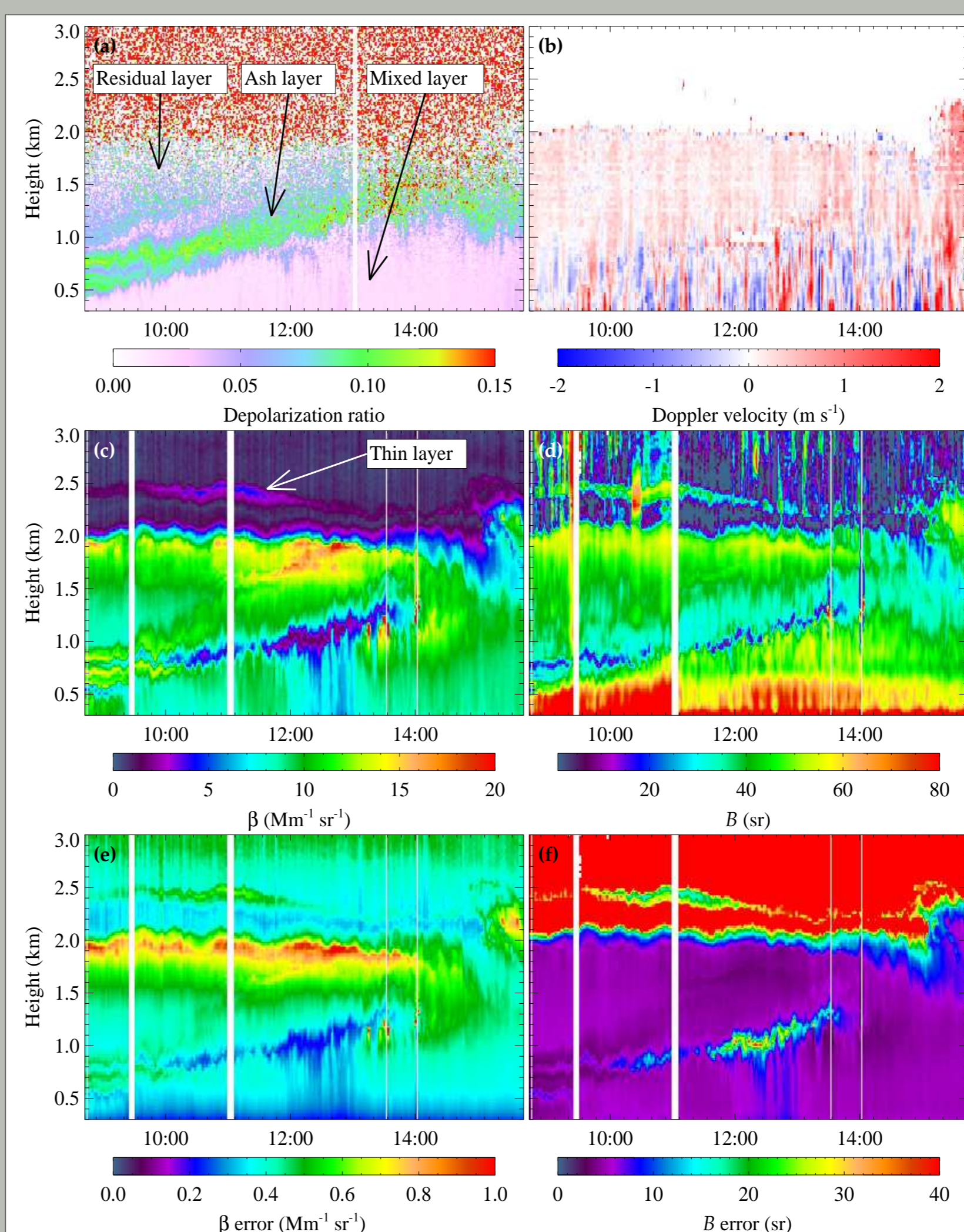
The previous retrievals, in extinction mode, including uncertainties (blue around a red line) compared to the traditional method (diamonds).

The total uncertainty returned by the retrievals is 2–20 %, shown above left for the previous simulations. That also compares the retrieval to results of the traditional Raman lidar technique [2], which are in good agreement in the PBL. The retrievals exhibit a lesser spread and uncertainty than the Raman solution, especially in the free troposphere. The Fernald-Klett method [3] gives equivalent answers if the correct lidar ratio is known.

## Practical application



Total backscatter (top) and two-way extinction (bottom) for six analogue profiles observed during March 2010. The attenuated backscatter coefficient reported by an independent lidar is shown (diamonds) for comparison. The scattering that would be observed from a clear atmosphere is shown in black, highlighting negative  $\alpha$  returned by the traditional technique.



Observations of the Eyjafjallajökull ash plume at on 19 April 2010. (a) Depolarization ratio. (b) Vertical velocity. (c) Backscatter retrieved in extinction mode. (d) Lidar ratio retrieved from same. (e–f) Uncertainties on (c–d).

Six profiles observed with the Chilbolton UV Raman lidar during March 2010 were processed, shown left and compared to results given by the Fernald-Klett and Raman methods. In the PBL, the retrievals are very similar to the Raman technique and measurement by an independent lidar. As the SNR decreases, the retrieval tends towards the Fernald-Klett solution. The resolution increases from 30 to 100 m for backscatter and 100 to 500 m for extinction. A tendency to find  $\alpha = 0$  at the top of the PBL is due to an error in the number density profile.

Below that are observations of Eyjafjallajökull ash on April 19th. Large depolarization ratios indicate the presence of a 400 m thick ash layer within the PBL, though the observed value of 0.1 is smaller than that expected for mineral dusts [4]. It exhibits a low backscatter ( $< 10 \text{ Mm}^{-1} \text{sr}^{-1}$ ) and lidar ratio (20–30 sr) compared to published values [5, 6] and those observed earlier at the same site. The decreased  $B$  could imply particle growth after 12–24 hours within the PBL (though Raman observations indicate the region is relatively dry).

A mixed layer forms beneath the ash where  $B = 50\text{--}80$  sr with minimal depolarization, which is broadly consistent with urban aerosols. A more weakly depolarizing aerosol resides in a poorly-mixed residual layer above the ash, which persists until they mix at 14:00. Backscatter and lidar ratios decrease with height. Larger particles may have begun to settle from this layer, though it does not seem that sufficient time has passed to produce so large a gradient.

It is desired to apply the retrieval to more data, especially instruments that have been thoroughly calibrated. The retrieval has been shown to perform at least as well as existing techniques and will be most powerful when applied with minimal extraneous uncertainty.

## References

Thanks to all the staff at CFARR for their data and assistance through the years and to P. Dreuw and T. Deselaers for the L<sup>A</sup>T<sub>E</sub>X style file.

- [1] C. Rodgers, *Inverse methods for atmospheric sounding*, World Scientific (2000).
- [2] A. Ansmann et al., *AO* 31(33), 7113–7131 (1992). doi:10.1364/AO.31.007113.
- [3] F. G. Fernald, *AO* 23(5), 652–653 (1984). doi:10.1364/AO.23.00652.
- [4] A. Ansmann et al., *JGR* 116, D00U02 (2011). doi:10.1029/2010jd015567.
- [5] F. Marengo and R. Hogan, *JGR* 116, D00U06 (2011). doi:10.1029/2010jd015415.
- [6] M. Hervo et al., *ACP* 12(4), 1721–1736 (2012). doi:10.5194/acp-12-1721-2012.